NeuroImage 45 (2009) 1040–1046

Contents lists available at ScienceDirect

NeuroImage

journal homepage: www.elsevier.com/locate/ynimg

Cross-frequency coupling of brain oscillations indicates the success in visual motion discrimination

Barbara Händel, Thomas Haarmeier *

Department of Cognitive Neurology, Hertie-Institute for Clinical Brain Research, University of Tübingen, Klinikum Schnarrenberg, Hoppe-Seyler-Straβe 3 72076 Tübingen, Germany
Department of General Neurology, Hertie-Institute for Clinical Brain Research, University of Tübingen, 72076 Tübingen, Germany

ARTICLE INFO

Article history:
Received 13 July 2008
Revised 17 October 2008
Accepted 5 December 2008
Available online 25 December 2008

ABSTRACT

Cortical activity such as recorded by EEG or MEG is characterized by ongoing rhythms that encompass a wide range of temporal and spatial scales. Recent studies have suggested an oscillatory hierarchy with faster oscillations being locked to preferred phases of underlying slower waves, a functional principle applied up to the level of action potential generation. We here tested the idea that amplitude-phase coupling between frequencies might serve the detection of weak sensory signals. To this end we recorded neuromagnetic responses during a motion discrimination task using near-threshold stimuli. Amplitude modulation of occipital high-frequency oscillations in the gamma range (63±5 Hz) was phase locked to a slow-frequency oscillation in the delta band (1–5 Hz). Most importantly, the strength of gamma amplitude modulation reflected the success in visual discrimination. This correlation provides evidence for the hypothesis that coupling between low- and high-frequency brain oscillations subserves signal detection.

Introduction

Activity of neuronal groups is characterized by ongoing rhythms that encompass a wide range of temporal and spatial scales and that are considered to play an important role in cognition (see: Steriade et al., 1996; Engel et al., 2001; Singer and Gray, 1995; Sejnowski and Paulsen, 2006; Buzsáki and Draghun, 2004; Ward, 2003; Basar et al., 2001; Klimesch, 1999; Fries, 2005; Varela et al., 2001). In the past, the functional significance of brain oscillations has usually been tested for the different frequency bands, separately. Neuronal processing, however, involves simultaneous oscillations in various frequency bands and recent studies have suggested an oscillatory hierarchy with faster oscillations being locked to preferred phases of underlying slower waves (Buzsáki, 2006; Canolty et al., 2006; Lakatos et al., 2005; Jensen and Colgin, 2007), a functional principle applied up to the level of action potential generation. A classic example of such co-variation is the hippocampus where single cell activity is modulated along with oscillating local field potentials (LFPs; O'Keefe and Recce, 1993) and oscillations in the gamma frequency range are amplitude-phase coupled to theta oscillations (Bragin et al., 1995; Buzsáki et al., 2003).

Co-modulation of various oscillations and single spikes is a feature not confined to the hippocampus. In monkey sensory cortex single cell responses have been found to be coupled to preferred phases of slow wave oscillations (Lee et al., 2005: visual cortex (area V4); Lakatos et al., 2005: auditory cortex) and cross-frequency coupling between slow frequency phase and fast frequency amplitude has been demonstrated in visual cortex (monkey: Lakatos et al., 2008; rabbit: Freeman and Rogers, 2002; cat: Volgushev et al., 2003) as well as auditory cortex (monkey: Lakatos et al., 2005). Also in humans amplitude-phase coupling between high gamma (80–150 Hz) and low frequency oscillations has been observed. In many studies this coupling was linked to memory tasks (Burgess and Ali, 2002; Schack et al., 2002). However, also other behavioral tasks not related to memory processes (namely auditory, visual and tactile) showed an amplitude/power modulation of gamma frequency by the phase of slow oscillations over various parts of the cortex (Canolty et al., 2006; Bruns and Eckhorn, 2004; Demiralp et al., 2007).

The functional significance of cross-frequency coupling between amplitude and phase has remained unclear. One possibility is that such coupling is important for input selection and, more specifically, might subserve the detection of weak sensory signals (Buzsáki, 2006). The reason is that the combination of fast and slow oscillations might facilitate spike generation in response to a given sensory input due to the dependency of action potential generation on even small, subthreshold electric field changes (Volgushev et al., 1998; Azouz and Gray, 2000; Radman et al., 2007; Francis et al., 2003). The goal of the present study was to test this idea by resorting to a visual motion discrimination paradigm which has been demonstrated recently to induce both high- (gamma, Siegel et al., 2007) and low- (delta, Händel et al., 2007, 2008) frequency oscillations.

* Corresponding author. Department of Cognitive Neurology, Hertie-Institute for Clinical Brain Research, University of Tübingen, Klinikum Schnarrenberg, Hoppe-Seyler-Straβe 3 72076 Tübingen, Germany. Fax: +49 7071 295326.
E-mail address: thomas.haarmeier@uni-tuebingen.de (T. Haarmeier).

1053-8119/$ – see front matter © 2008 Elsevier Inc. All rights reserved.
doi:10.1016/j.neuroimage.2008.12.013

Methods

Experimental design

Seven healthy subjects, 3 males and 4 females with a mean age of 29 (±2.9) years participated in this study. All subjects had normal or corrected to normal vision. Informed consent was obtained from all subjects according to the Declaration of Helsinki and the guidelines of the local ethics committee of the medical faculty of the University of Tübingen, which approved the study.

Subjects were seated upright in a magnetically shielded room (Vakuum-Schmelze, Hanau, Germany) during the magnetoencephalographic (MEG) recording. Stable posture was supported by a chinrest attached to the MEG chair. The computer generated visual stimuli were rear projected onto a large translucent screen (DLP-projector (digital light processing), frame rate 60 Hz, 800×600 pixel) positioned at a viewing distance of 92 cm in the magnetically shielded room. Viewing was binocular.

The visual stimulus consisted of 5 periods, each lasting 500 ms (see Fig. 1a). During the first 500 ms, only a stationary red dot (diameter 10 minarc) was presented in the middle of the screen which served as the fixation target and which remained visible until arrow onset (2.0 s). The first 500 ms period was followed by a second one introducing a random dot kinematogram (RDK) which covered a square of 16×16° and was centred 15° right of the fixation point. The RDK consisted of 1500 white squares (side length=8 arcmin, lifetime=1000 ms, dot density ~6dots/deg^2, luminance 47cd/m^2) all moving incoherently, i.e. in all possible directions with a resolution of 1°, at a common speed of 6°/s. After the presentation of this first RDK, a second RDK, the "test stimulus", started with properties identical to those described for the previous stimulus period except that a certain amount of dot elements now moved coherently in the same direction (either to the left or to the right). Specifically, the percentage of coherently moving dots was dependent on the individual threshold of the subject determined as will be described below. After a subsequent second fixation period, an arrow was presented in the middle of the screen pointing either to the left or to the right side as randomly chosen by the stimulus generator.

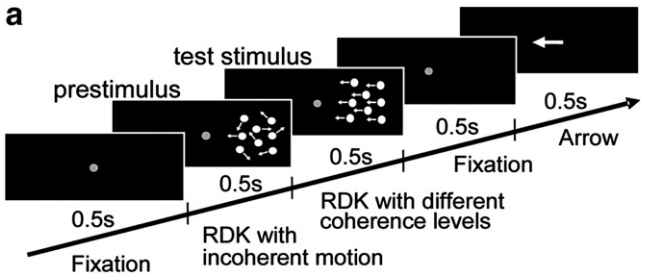

b

subjects	1	2	3	4	5	6	7
% correct responses	63	59	65	68	60	57	71
% motion coherence	7	6	24	11	14	14	14

Fig. 1. Time course of the stimulus and stimulus specifications for the different subjects. (a) The stimulus consisted of 5 periods each lasting 500 ms. In contrast to the "prestimulus", a random dot kinematogram (RDK) consisting of incoherent motion, the following "test stimulus" involved the presentation of coherent motion the percentage of which was adjusted in each subject in order to obtain ~65% correct responses. Coherent motion was directed either to the left or to the right. Subjects had to indicate whether the motion direction of the coherently moving dots of the test stimulus was identical or opposite to the pointing direction of the arrow presented at the end of the trial. Subjects viewed the stimuli during controlled stationary fixation. (b) Percentage of correct responses and amount of motion coherence (percentage of coherently moving dots) used for stimulation are listed for each of the seven subjects separately.

Subjects were instructed to indicate whether the motion direction of the dots of the test stimulus was identical (lifting right index finger) or opposite (lifting left index finger) to the pointing direction of the arrow (forced choice). Finger movements were detected using a light barrier. The individual threshold was identified beforehand by using a set of trials modulated by a staircase procedure in which the coherence level was varied until 65% of all trials were answered correctly. This coherence level was then used for stimulation during MEG recording.

During all experiments, eye movements were monitored using a homemade video system taking the pupil's center as measure of eye position. Recordings were stored at a sampling rate of 50 Hz and analyzed offline. In particular, oculomotor parameters like eye velocity, eye position and number and amplitude of saccades were tested for differences between correctly and incorrectly answered trials using *t*-statistics.

Recording of the MEG signals

Neuromagnetic activity was recorded using a whole-head MEG system (CTF Inc., Vancouver, Canada) comprising 151 first-order magnetic axial gradiometers. The signals were sampled at a rate of 625 Hz. Recording epochs lasted from stimulus onset to arrow offset plus 200 ms, leaving 2700 ms of recording time for each trial (420 single trials per subject). The subject's head position was determined at the beginning and at the end of each recording session by means of localization coils fixed to the nasion and preauricular positions to ensure that head movements did not exceed channel separation. Trials showing movement artifacts were detected by visual inspection and excluded. For frequency analysis baseline correction was performed by subtracting the mean of the whole stimulus period for each channel, separately. For analysis of the stimulus induced global field, recordings were baseline corrected by subtracting the time period from 240 to 499 ms after stimulus onset, i.e. the last 259 ms of initial fixation.

Global field analysis

In order to asses the global field activity, the root of the mean squared magnetic field (RMS) was calculated for each subject, each sensor and each sample separately. On single sensor basis, RMS values were then averaged for correctly and incorrectly answered trials and a paired *t*-test (correct vs. incorrect) was calculated over 6 consecutive samples and the group of 7 subjects (MATLAB, version 6.5.1). The time window (6 samples corresponding to ~10 ms) was shifted from 500 ms to 2400 ms in steps of 1 sample (sliding time window). Those sensors were considered to reveal a significant difference in RMS between correct and incorrect trials which continuously exhibited *p*-values below 0.001 during any 300 ms epoch (=31 consecutive samples). In order to be significant, differences between RMS values had to be present not only for consecutive samples (e.g. Fell et al., 2001) but also for two neighboring sensors.

Frequency analysis

Spectral analyses were performed on two frequency bands. The frequency of the slow wave was chosen on the basis of a previous experiment which had shown a strong prevalence of 3±2 Hz oscillations for the same motion paradigm (Händel et al., 2007). The gamma band around 63 Hz (±5 Hz) was chosen because of a pronounced peak in the power spectrum. MEG recordings were Gaussian filtered (i.e. FIR filter applied as a convolution with a Gaussian in the frequency domain) for the two frequency bands (i.e. 3±2 Hz and 63±5 Hz, respectively) on a single trial basis. Data was amplitude demodulated by means of a Hilbert transformation, and trials were averaged over the two different categories (correct versus

incorrect). The further analysis was conducted for the time period ranging from 500 to 2400 ms after stimulus onset. Amplitude values obtained from this time period were compared between correct and incorrect trials on single sensor basis using a *t*-test across the Hilbert transformed amplitude values.

In order to improve the temporal resolution of the analysis, spectral amplitudes in the two frequency ranges were also tested based on sliding time windows. As described for the RMS values, a *t*-test comparing correct and incorrect trials was calculated for the group of 7 subjects and for each sensor. This time, *t*-tests were based on single samples because, due to filtering, neighboring samples were no longer independent. Sensors were taken to reveal significant differences in spectral amplitude between conditions when all *p*-values of any 300 ms epoch (=187 consecutive samples) would meet a criterion of $p<0.05$. The epoch was moved across the whole time period of stimulation in steps of single samples as described above. Again, two neighboring sensors had to be significant.

Analysis of gamma amplitude during delta peaks vs. delta troughs

To analyze cross-frequency coupling we tested in a first approach if the amplitudes of the gamma oscillation would be different during the peaks of the delta wave compared to the delta troughs (Canolty et al., 2006). Single trial data shown later in the results (cf. Fig. 4) illustrate this approach. To this end we extracted for each trial separately the Hilbert modulated amplitude values of the gamma band for those points in time for which the delta phase of the given trial would be within a range of 0±pi/12 (covering the peak in the delta wave) or would meet the trough criterion (phase>pi−pi/12 & <−pi+pi/12). The only requirement for a given single trial to be accepted was that at least one full circle of delta had to be present, i.e. 34 samples (=55.5 ms) had to fulfill peak and trough criteria, respectively, as defined before. Gamma amplitude values were now averaged separately for the peaks and troughs leaving us with one (mean) peak and one (mean) trough value for each trial, each sensor and each subject. Trials were further sorted for correctly answered trials and incorrectly answered ones. Since the percentage of correctly answered trials was expected and indeed turned out to be higher than 50%, we matched the number of trials using a randomization process. A group statistic (*t*-test over 7 subjects) was now calculated for each sensor comparing the peak values with the trough values within each group of trials (correct and incorrect trials), separately. The *p* levels taken to be significant were adjusted by means of a Bonferroni correction given that the *p* values of two adjacent sensors had to be significant (*p*_corrected=sqrt(0.05/151 sensors)=0.018).

To exclude the possibility that movement artifacts influenced the results we computed the identical analysis as before but now using 120±10 Hz as filter frequency, a frequency often found to be prevalent during movements.

Cross correlation between delta signal and gamma amplitude modulation

In order to further characterize the temporal dependency between the gamma and delta oscillations we calculated on single trial basis a cross correlation (temporal resolution: 1.6 ms) between the 3 Hz signal and the gamma amplitude modulation (Hilbert transformed gamma amplitude). This analysis was confined to those sensors which had revealed significant peak-trough differences. The maximal correlation coefficient and the corresponding phase shift were extracted for each trial and grouped dependent on the answer (correct or incorrect). Since we had more correctly compared to incorrectly answered trials we again balanced the number of trials as described in the previous section. The upper 5% of the maximal correlation coefficients were now compared between groups of correct and incorrect trials (two-sided *t*-test).

Results

Behavioral performance

Subjects performed a visual motion discrimination task in which the direction of coherently moving dots embedded in noise had to be discerned (Fig. 1). The visual configuration of the task was chosen to be demanding. On average 63±5% of the trials were answered correctly with the mean motion coherence being 13±6%. Fig. 1b shows an overview of the coherence levels applied and the resulting percentages of correctly answered trials obtained in the MEG experiment. For each of the subjects the percentage of correctly answered trials was higher than 50% showing that discrimination, albeit demanding, was better than chance level.

Analyses of eye movements recorded with a video system did not show any significant difference between correctly and incorrectly answered trials for the different oculomotor parameters considered such as slow eye drifts (eye velocity), deviations from the fixation point (eye position) or the number and amplitude of saccades ($p>0.05$, each). Incorrect responses, therefore, did not reflect differences in oculomotor strategy. Importantly, the lack of oculomotor influences also ensured that differences in the MEG responses would not reflect differences in retinal stimulation.

Evoked responses

Statistical analysis of the global field induced revealed an increase in activity for correct as compared to incorrect trials. As shown in Fig. 2a plotting the global field power (GFP), i.e. the RMS values averaged across all sensors, this difference developed shortly after test stimulus onset. It was mostly caused by two foci, a first one located in contralateral (left) parieto-occipital cortex and a second one more widely distributed over frontal cortex (Fig. 2b). Activity recorded from parieto-occipital sensors significantly differentiated between correct and incorrect trials shortly after coherent motion onset, i.e. at a latency of 180 ms, and stayed significant for a total of 425 ms (Fig. 2a). The second focus with significant differences, observed over five frontal sensors, also showed higher RMS values during correct trials but reached significance 268 ms later (latency 448 ms). This second differential activity persisted 186 ms reaching into the fixation period following the coherent motion presentation (Fig. 2a). During all other stimulus epochs no significant difference was observed.

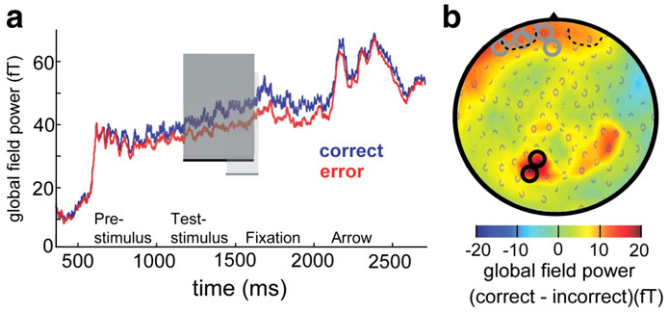

Fig. 2. Relationship between the global magnetic field induced and the success in visual motion discrimination. (a) Global field power, i.e. the RMS amplitudes averaged over all sensors and the 7 subjects, plotted for correctly (blue) and incorrectly (red) answered trials as function of time. Transparent bars mark the time periods during which at least two neighboring sensors exhibited a significant difference between correct and incorrect trials (black: 1180–1605 ms, grey: 1448–1634 ms). The color of the bars corresponds to the color of sensors marked in b. (b) Amplitude differences between correctly and incorrectly answered trials, averaged over the time period for which any group of sensors revealed significant differences (1180–1634 ms). Amplitude differences are projected onto a two-dimensional MEG sensor map (seen from above, nose up). Yellow to red colors signify that amplitudes are higher for correctly answered trials, blue colors signify the opposite. Circles mark the position of sensors showing significant differences between the two types of trials.

Oscillatory responses

Frequency analysis showed strong oscillations in both the delta (3±2 Hz) and in the gamma band (63 ±5 Hz). These oscillations were observed over a broad range of sensors as can be seen in Fig. 3 plotting the group data. While the delta oscillation showed peak amplitudes in sensors located over bilateral occipital and temporal cortex (Fig. 3b), the gamma oscillations were more clustered around the occipital pole (Fig. 3a). As evident from Fig. 3 differences in the distribution or strength of the oscillations between correctly versus incorrectly answered trials were rather small. In fact, amplitudes did not show a significant difference between the two conditions for neither of the two spectra and for none of the 151 sensors (*t*-test applied on the spectral amplitudes) if the time interval of the whole stimulus except first fixation period was considered (500 ms–2500 ms).

As explained in the Methods section, spectral amplitudes between conditions were also compared for sliding segments of 300 ms in order to improve temporal resolution of the analysis. While this analysis did not reveal any significant differences in the gamma spectrum, small effects were observed for the 3 Hz oscillation (Fig. 3c). Specifically, there was an overall tendency for smaller spectral amplitudes for correct as compared to incorrect trials which reached the level of statistical significance at three separate points in time. At a latency of 1107 ms, i.e. 107 ms after test stimulus onset, this difference was significant in two parieto-occipital sensors and lasted for 313 ms. A second and a third set of sensors showed differences in spectral power following the second fixation period. Specifically, four frontal sensors (latency 1981 ms) showed significance for 317 ms and two further temporo-occipital sensors (latency 2374 ms) were significant for 248 ms. All the three effects were small (compare again Fig. 3c),

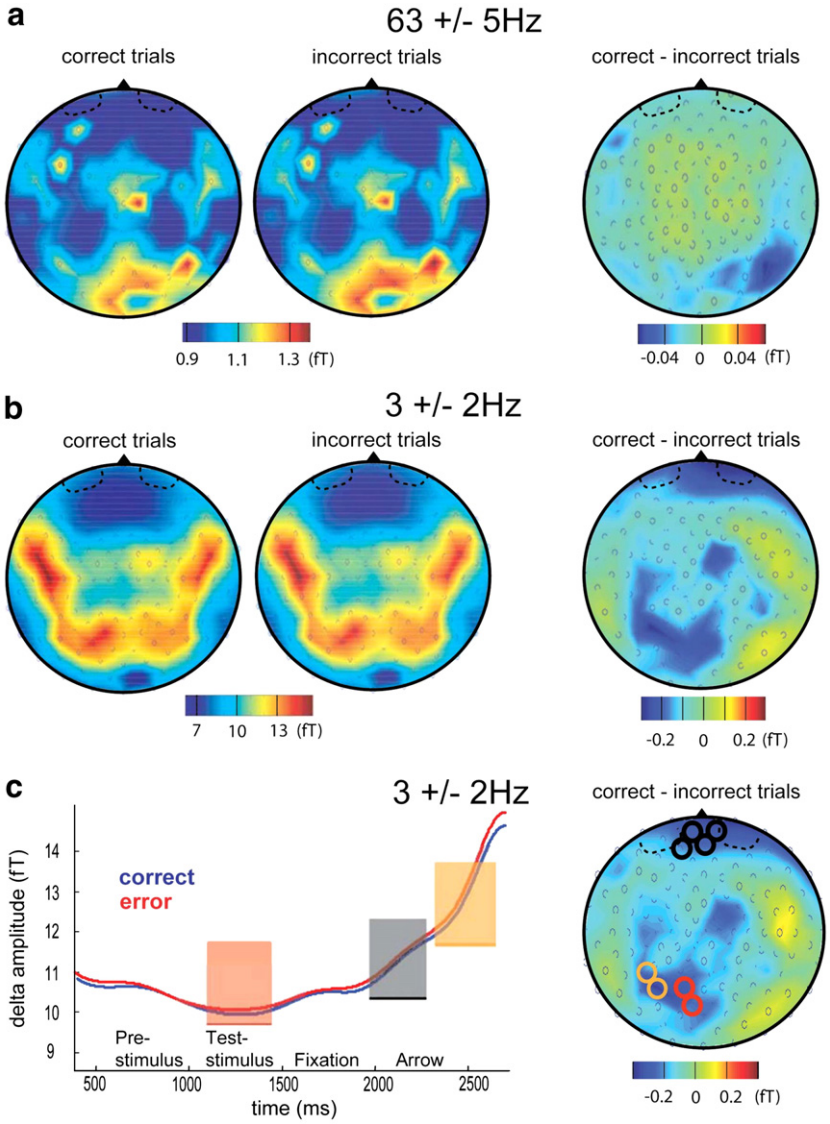

Fig. 3. Spatial distribution and amplitudes of the low-frequency (3 Hz) and the high-frequency (63 Hz) signals depicted for correct and incorrect trials. (a) Amplitude values of the 63±5 Hz frequency band averaged for the group of subjects over all correctly answered trials (on the left) and all incorrectly answered trials (in the middle) as well as their differences (on the right), projected onto two-dimensional MEG sensor maps (seen from above, nose up; time window: 500–2500 ms after stimulus onset). (b) Amplitude values of the 3±3 Hz frequency band, same conventions as in a. (c) Analysis of the 3 Hz signal based on sliding time windows of 300 ms. The mean amplitude of the 3 Hz signal averaged over the 7 subjects and all sensors plotted for correctly (blue) and incorrectly (red) answered trials and plotted as function of time (left panel). Transparent bars mark the time periods in which at least two neighboring sensors exhibited a significant difference between conditions (black: 1981–2298 ms; red: 1107–1420 ms; orange: 2374–2622 ms). The color of the bars correspond to the color of the circles in the two-dimensional MEG sensor map (right) marking sensor positions with significant differences. Amplitude differences of the 3±2 Hz frequency band between correctly and incorrectly answered trials are averaged here from 1107 to 2622 ms, i.e. the period covering statistically significant events.

and all three effects had the same sign, i.e. they revealed smaller amplitudes for correct as compared to incorrect trials.

Cross-frequency coupling

The comparison of correct and incorrect trials revealed qualitative differences when interactions between the two spectra, i.e. cross-frequency coupling, was considered. As exemplified in Fig. 4 for a single trial, delta oscillation and gamma amplitudes were co-modulated. The delta response in this trial oscillates at a certain phase while in the same sensor and during the same trial also gamma oscillations are present (Figs. 4a, b). The gamma response is modulated considerably in amplitude as captured by the envelope, i.e. the Hilbert transformed curve. Superposition of the delta phase and the gamma envelope reveals that (in this trial) high amplitudes in the gamma range tend to coincide with troughs of the delta wave (Fig. 4c). This impression was corroborated by statistical analysis testing for significant differences in gamma amplitudes present during the peaks of the delta waves on the one hand and those recorded during delta troughs on the other hand (Fig. 5). For correct trials, the differences were locally clustered around occipital sensors with increased gamma amplitudes during the delta troughs as compared to the peaks (Fig. 5a, left map). In other sensors, these differences were virtually absent. Statistical analysis confirmed that the modulation of occipital gamma amplitude was significant as indexed by 4 neighboring sensors meeting the criterion of $p<0.018$ (Fig. 5b, left map). In contrast, in incorrect trials the spatial distribution of gamma amplitude modulation was rather incoherent (Fig. 5a, right map). On the one hand, the occipital gamma modulation appeared to be weaker as compared to correct trials and on the other hand, several other sensors reaching up to frontal cortex showed modulations of the gamma amplitude. None of the modulation peaks, however, reached the level of statistical significance. Specifically, only one single sensor in the left precentral area met the statistical criterion of $p<0.018$ but did not survive correction for multiple comparison since neighboring sensors did not show the same effect (Fig. 5b, right map).

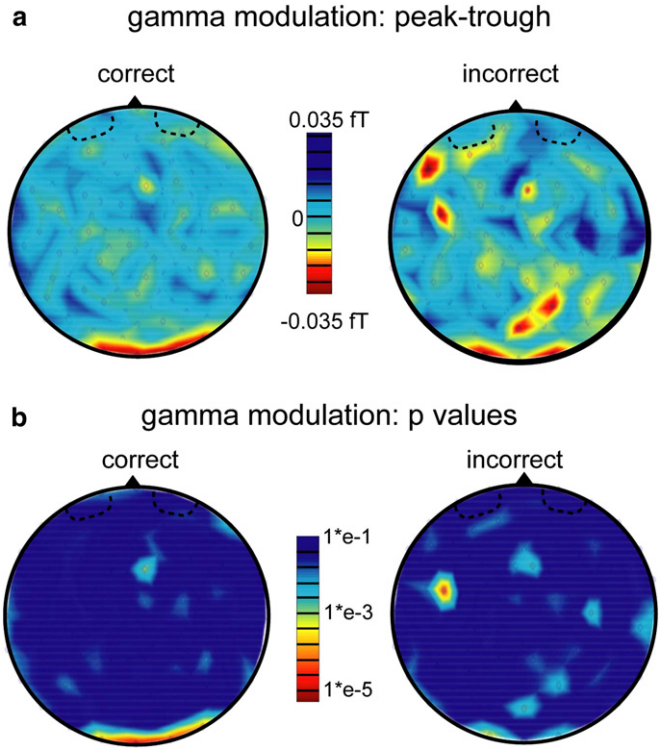

Fig. 5. Spatial distribution of gamma amplitude modulation co-varying with delta phases. (a) Magnetic field map of the group difference between gamma amplitudes obtained for the delta peaks versus the delta troughs. Amplitude values were averaged for the group of subjects over all correctly answered trials (on the left) and all incorrectly answered trials (on the right) and projected onto a two-dimensional MEG sensor map (seen from above, nose up; time window: 500–2500 ms after stimulus onset). Warm colors signify that gamma amplitudes collected during delta troughs are higher than those during delta peaks, blue colors signify the contrary. (b) Statistical probability mapping of gamma amplitude dependency on delta phase projected onto the same two-dimensional MEG sensor map shown in a. *P* values denoting the level of statistical significance of the gamma amplitude difference (shown in a) were calculated from *t*-tests and are color-coded here in order to provide a quasi-field distribution.

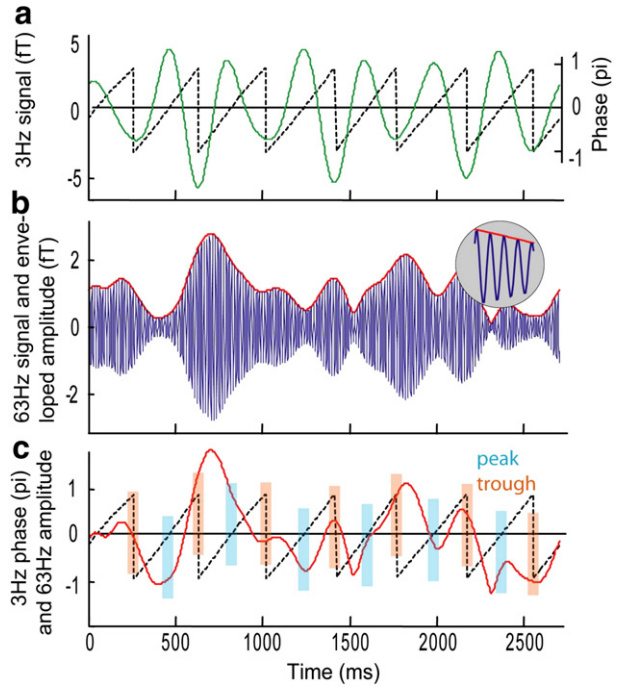

Fig. 4. Relationship between gamma amplitude and delta phase shown for an exemplary trial and sensor. (a) The delta signal (3±2 Hz) (green solid line) and its corresponding phase (black broken line, between +pi and −pi, *y*-axis on the left) are plotted over the whole time of stimulus presentation. (b) The gamma oscillation of the same trial (blue solid line, the inset shows an enlargement of a short time period). The change in amplitude as identified by a Hilbert transformation is depicted in red. (c) The change in gamma amplitude (red line, same as depicted in b) and the phase of the delta oscillation (black broken line, same as in a) superimposed on each other. The *y*-axis shows the pi values for the phase. Amplitude values of the gamma signal are arbitrary since for clarity the curve has been shifted and magnified. Delta peaks (phase values between 0±pi/12) and the corresponding gamma amplitudes are marked with blue squares, troughs (phase >pi−pi/12 & <−pi+pi/12) with red squares.

In order to control for possible influences of head movements involving EMG activity of neck muscles and in order to also test for the frequency specificity of the effect in the gamma range, we performed the same analysis on responses in a higher frequency range (120± 10 Hz). No significant difference between peak and trough was found ($p>0.1$ for each sensor).

Cross-correlations were calculated on single trial basis between the delta signal and gamma amplitude modulation for those four occipital sensors that had shown a significant effect in the first analysis. Based on these cross-correlations the maximal correlation coefficients with their corresponding time shifts were extracted. Fig. 6a shows the difference (correct−incorrect) between the normalized probability of these correlation coefficients plotted in three bins. Values in the highest bin (0.56–0.8) were positive, indicating a greater number of high correlation coefficients for correct as compared to incorrect answers, whereas values of the lowest bin (0.08–0.32) were negative showing a higher number of incorrect trials with low correlation coefficients. On the other hand, intermediate correlation coefficients (middle bin, 0.32–0.56) were observed equally often in both types of trials. The preference for high correlation coefficients in

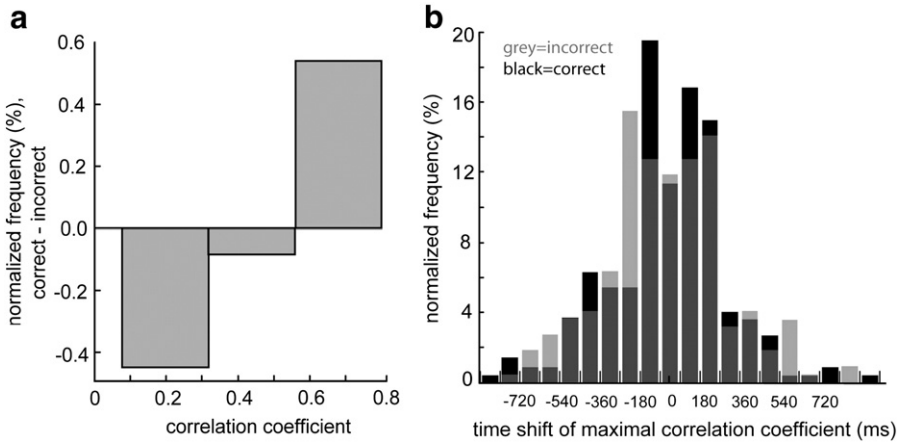

Fig. 6. Cross-frequency coupling as assessed by cross correlation between gamma amplitude and delta phase. a. Probabilities of correlation coefficients observed for correct as compared to incorrect trials: difference (correct minus incorrect) of observed frequency of occurrence plotted for three different ranges/bins of correlation coefficients (i.e. 0.08–0.32, 0.32–0.56, 0.56–0.8). Positive values denote higher frequencies of occurrence in correct trials and vice versa. b. Frequency distribution of the time shifts for which the maximal correlation coefficient within a given trial was observed. This distribuition is based on the 5% of trials showing the highest correlation coefficients within the two groups of trials (correct trials: black; incorrect trials: grey). Time bins are equally spaced and span at total of 90 ms each. Based on a main frequency of 3 Hz, a time period of 83 to 249 ms corresponds to the trough of delta, and a period from 0 to 83 ms and 249 to 333 ms corresponds to the peak.

correctly as compared to incorrectly answered trials was also indicated by the fact that the maximum coefficients were observed in the first. Specifically, the highest 5% of correlation coefficients obtained from correct trials averaged 0.61 while amounting to 0.59 in incorrect trials ($p<0.0001$; t-test over all subjects, trials and the 4 sensors).

Fig. 6b plots the distribution of the time shifts of maximal correlation coefficient of those 5% of trials showing the highest correlation coefficients of the four sensors selected. Correlation coefficients with a corresponding phase shift of 0 ms would indicate that gamma amplitude modulation and delta waves coincided with zero time lag, i.e. that gamma amplitude was highest during the delta peak. As can be seen in Fig. 6b the frequency of time shifts of the maximal correlation coefficient (ms) peaked left and right of zero in time bins ranging from −270 to −180/−180 to −90 ms and from 90 to 180/180 to 270 ms, respectively. Since one full delta (3 Hz) circle corresponded to 333 ms, this phase shift indicates a displacement of about half the delta circle, i.e. gamma amplitudes were highest during the delta trough, a tendency already indicated by the first analysis. This phase preference was prevalent for both the correct as well as the incorrect trials, however, phase preference appeared much stronger in correct trials as indicated by two prominent peaks.

Discussion

Magnetoencephalographic or electroencephalographic recordings of the human brain are characterized by ongoing rhythms that encompass a wide range of temporal and spatial scales (Buszáki and Draguhn, 2005). How oscillations of different frequency bands might influence each other is an important question given the simultaneous presence of multiple oscillators in various parts of the brain (Buzsáki, 2006; Canolty et al. 2006). Recent studies have suggested an oscillatory hierarchy with faster oscillations being locked to preferred phases of underlying slower waves (Lakatos et al., 2005; Canolty et al., 2006). It has been hypothesized that cross-frequency coupling might be important to improve long-range communication in such a way that local processing is facilitated during time windows of increased excitability defined by specific phases of the underlying lower frequency which might manifest itself in a phase-amplitude locking. Combination of the two oscillators might, thus, increase the magnitude of input variability so that a weak, subthreshold input might become effective in discharging a critical number of target neurons. Along this line of arguments and based on the observation that amplitude fluctuations in the gamma frequency band in visual cortex are phase-locked to the depolarization peaks of membrane potential changes in the delta frequency range, Volgushev et al. (2003) speculated that phase-locking might provide visual cortex neurons with the possibility to exploit the advantages of stochastic resonance (Volgushev et al., 2003; Wiesenfeld and Moss, 1995; Anderson et al., 2000; Volgushev and Eysel, 2000) in the detection of weak visual signals. The main result of the present study yields clear evidence in favor of this functional interpretation. It was the amount of cross-frequency coupling which was related to the success in visual discrimination with increased strength of coupling for correctly compared to incorrectly answered trials.

Albeit analyzed only occasionally so far, cross-frequency locking between delta phase and the amplitude of gamma oscillations is not without precedent in the literature and has been found between slow oscillations in a range of 0.1 to 10 Hz and gamma oscillations in a range of 20 to 100 Hz in animal (Lakatos et al., 2008; Lakatos et al., 2005; Freeman and Rogers, 2002; Volgushev et al., 2003) as well as human studies (Bruns and Eckhorn, 2004; Demiralp et al., 2007) within the visual cortex. The frequencies as well as the location, i.e. sensors over the occipital pole which exhibited cross-frequency coupling in this study, therefore, are in good agreement with previous results. Also the delta phase which the gamma modulation was locked to agrees with findings of previous studies. Our data showed an increase in amplitude of gamma oscillation during the trough of delta wave, correspondent to a phase lag of about half the delta cycle. Phase lags in former studies were ranging roughly between 1/3 pi and pi (Lakatos et al., 2005; Demiralp et al., 2007).

While the phenomenon of amplitude-phase coupling across frequencies per se is well established, the present study suggests a direct link to perception, i.e. the success in visual motion discrimination. It is important to note that there was no indication of confounding factors that could have induced changes in coupling unrelated to perception. The reason is that none of the behavioral parameters controlled by the paradigm except the success in discrimination showed significant differences between the two conditions compared. Specifically, eye movements were not significantly different for the two types of trials and also analysis of high-frequent gamma band activity (120±10 Hz), i.e. a frequency band typically resulting from movements through muscle contraction, did not contribute to the cross-frequency coupling analyzed here.

One may ask whether the low frequency band might have been introduced by slow changes in the evoked field which would lead to

power increases in a broad frequency band possibly mimicking intrinsic oscillations. Rodriguez and Valdes-Sosa (2006) showed that evoked potentials, attributed to extrastriate cortex, start to differentiate between correct and incorrect trials at around 200 ms after stimulus onset with larger amplitudes for correctly identified motion directions. Also in the study at hand, analysis of global field activity revealed responses from contralateral parieto-occipital sensors as well as frontal sensors to be higher in correct trials. Importantly, this kind of analysis, when applied to the delta frequency band, showed the opposite effect, namely a decrease in power, albeit small, for correct compared to incorrect trials. These opposing effects, i.e. the increase in global field power on the one hand and the decrease in delta amplitude on the other hand, indicate that power changes in the delta band were not directly related to the overall evoked field activity. Interestingly, amplitudes in this frequency band seem to reflect the attentional state of the observer during target presentation (Händel et al., 2008). Since it is plausible to assume that also in the present task attentional effects were the main cause for perceptual differences, the observed decrease in amplitude for correct trials is in good agreement with the results reported recently for stimuli employing low motion coherence (Händel et al., 2008).

The finding of lower delta amplitudes for correct as compared to incorrect trials is also important with respect to a remaining concern not addressed so far, namely the possibility that the difference in cross-frequency coupling between conditions might be secondary to a change in power of one of the two contributing frequencies. Although power of each of the two oscillations did not differentiate between conditions when analyzed over the whole time period in which cross-frequency coupling was assessed, analysis with higher temporal resolution revealed, as mentioned above, small differences in the delta spectrum which were absent in the gamma frequency range. Besides the fact that significant differences in coupling were found at quite a distinct localization as compared to the main effects in delta power, also the sign of the delta effects does not support the notion that differences in coupling were due to changes in delta power: if anything, coupling would be expected to decrease with smaller delta amplitudes.

Although it is not possible to directly infer from our results whether cross-frequency amplitude-phase coupling was related to the detection of coherent motion, i.e. the percept, or a process related to working memory, its dominance in the posterior sensors suggests a mechanism close to visual signal detection. We, therefore, interpret our results in line with the hypothesis that the responsiveness of neurons to incoming sensory signals is not entirely determined by the signal itself but also by oscillatory fluctuations in the neuronal network. More specifically, the present results support the concept that coupling of different cortical oscillators plays a constructive role in the detection of weak signals.

Acknowledgments

We thank W. Lutzenberger for many helpful discussions. The work was supported by the DFG (SFB 550, TP A2) and the Hertie Foundation.

References

Anderson, J., Lampl, I., Gillepsie, D.C., Ferster, D., 2000. The contribution of noise to contrast invariance of orientation tuning in cat visual cortex. Science 290, 1968–1972.
Azouz, R., Gray, C.M., 2000. Dynamic spike threshold reveals a mechanism for synaptic coincidence detection in cortical. Proc. Natl. Acad. Sci. 97, 8110–8115.
Basar, E., Basar-Eroglu, C., Karakas, S., Schürmann, M., 2001. Gamma, alpha, delta, and theta oscillations govern cognitive processes. Int. J. Psychophysiol. 39, 241–248.
Bragin, A., Jando, G., Nddasdy, Z., Hetke, J., Wise, K., Buzsaki, G., 1995. Gamma (40–100 Hz) oscillation in the hippocampus of the behaving rat. J. Neurosci. 15, 47–60.
Bruns, A., Eckhorn, R., 2004. Task-related coupling from high- to low-frequency signals among visual cortical areas in human subdural recordings. Int. J. Psychophysiol. 51, 97–116.
Burgess, A.P., Ali, L., 2002. Functional connectivity of gamma EEG activity is modulated at low frequency during conscious recollection. Int. J. Psychophysiol. 46, 91–100.
Buzsáki, G., 2006. Rhythms of the Brain. Oxford University Press, New York.
Buzsáki, G., Draghun, A., 2004. Neuronal oscillations in cortical networks. Science 304, 1926–1929.
Buzsáki, G., Buhl, D.L., Harris, K.D., Csicsvari, J., Czeh, B., Morozov, A., 2003. Hippocampal network patterns of activity in the mouse. Neuroscience 116, 201–211.
Canolty, R.T., Edwards, E., Dalal, S.S., Soltani, M., Nagarajan, S.S., Kirsch, H.E., 2006. High gamma power is phase-locked to theta oscillations in human neocortex. Science 313, 1626–1628.
Demiralp, T., Bayraktaroglu, Z., Lenz, D., Junge, S., Busch, N.A., Maess, B., Ergen, M., Herrmann, C.S., 2007. Gamma amplitudes are coupled to theta phase in human EEG during visual perception. Int. J. Psychophysiol. 64, 24–30.
Engel, A.K., Fries, P., Singer, W., 2001. Dynamic predictions: oscillations and synchrony in top–down processing. Nat. Rev., Neurosci. 2, 704–716.
Fell, J., Klaver, P., Lehnertz, K., Grunwald, T., Schaller, C., Elger, C.E., Fernández, G., 2001. Human memory formation is accompanied by rhinal–hippocampal coupling and decoupling. Nat. Neurosci. 4 (12), 1259–1264.
Francis, J.T., Gluckman, B.J., Schiff, S.J., 2003. Sensitivity of neurons to weak electric fields. J. Neurosci. 23, 7255–7261.
Freeman, W.J., Rogers, L.J., 2002. Fine temporal resolution of analytic phase reveals episodic synchronization by state transitions in gamma EEGs. J. Neurophysiol. 87, 937–945.
Fries, P., 2005. A mechanism for cognitive dynamics: neuronal communication through neuronal coherence. Trends Cogn. Sci. 9, 474–480.
Händel, B., Lutzenberger, W., Thier, P., Haarmeier, T., 2007. Opposite dependencies on visual motion coherence in human area MT+ and early visual cortex. Cereb. Cortex 17, 1542–1549.
Händel, B., Lutzenberger, W., Thier, P., Haarmeier, T., 2008. Selective attention increases the dependency of cortical responses on visual motion coherence in man. Cereb. Cortex 18, 2902–2908.
Jensen, O., Colgin, L.L., 2007. Cross-frequency coupling between neuronal oscillations. Trends Cogn. Sci. 11 (7), 267–269.
Klimesch, W., 1999. EEG alpha and theta oscillations reflect cognitive and memory performance: a review and analysis. Brain Res. Rev. 29, 169–195.
Lakatos, P., Shah, A.S., Knuth, K.H., Ulbert, I., Karmos, G., Schroeder, C.E., 2005. An oscillatory hierarchy controlling neuronal excitability and stimulus processing in the auditory cortex. J. Neurophysiol. 94, 1904–1911.
Lakatos, P., Karmos, G., Mehta, A.D., Ulbert, I., Schroeder, C.E., 2008. Entrainment of neuronal oscillations as a mechanism of attentional selection. Science 320, 110–113.
Lee, H., Simpson, G.V., Logothetis, N.K., Rainer, G., 2005. Phase locking of single neuron activity to theta oscillations during working memory in monkey extrastriate visual cortex. Neuron 45, 147–156.
O Keefe, J., Recce, M.L., 1993. Phase relationship between hippocampal place units and the EEG theta rhythm. Hippocampus 3, 317–330.
Radman, T., Su, Y., An, J.H., Parra, L.C., Bikson, M., 2007. Spike timing amplifies the effect of electric fields on neurons: implications for endogenous field effects. J. Neurosci. 27, 3030–3036.
Rodriguez, V., Valdes-Sosa, M., 2006. Sensory suppression during shifts of attention between surfaces in transparent motion. Brain Res. 1072, 110–118.
Schack, B., Vath, N., Petsche, H., Geissler, H.-G., Möller, E., 2002. Phase-coupling of theta-gamma EEG rhythms during short-term memory processing. Int. J. Psychophysiol. 44Z, 143–163.
Sejnowski, T.J., Paulsen, O., 2006. Network oscillations: emerging computational principles. J. Neurosci. 26 (6), 1673–1676.
Siegel, M., Donner, T.H., Oostenveld, R., Fries, P., Engel, A.K., 2007. High-frequency activity in human visual cortex is modulated by visual motion strength. Cereb. Cortex 17, 732–741.
Singer, W., Gray, C.M., 1995. Visual feature integration and the temporal correlation hypothesis. Annu. Rev. Neurosci. 18, 555–586.
Steriade, M., Contreras, D., Amzica, F., Timofeev, I., 1996. Synchronisation of fast (30–40 Hz) spontaneous oscillations in intrathalamic and thalamocortical networks. J. Neurosci. 16, 2788–2806.
Varela, F., Lachaux, J.P., Rodriguez, E., Martinerie, J., 2001. The Brainweb: phase synchronization and large-scale intergration. Nat. Rev., Neurosci. 2, 229–239.
Volgushev, M., Eysel, U.T., 2000. Noise makes sense in neuronal computing. Science 290, 1908–1909.
Volgushev, M., Chistiakova, M., Singer, W., 1998. Modification of discharge patterns of neocortical neurons by induced oscillations of the membrane potential. Neuroscience 83, 15–25.
Volgushev, M., Pernberg, J., Eysel, U.T., 2003. γ-Frequency fluctuations of the membrane potential and response selectivity in visual cortical neurons. Eur. J. Neurosci. 17, 1768–1776.
Ward, L.M., 2003. Synchronous neural oscillations and cognitive processes. Trends in Cog. Science 7, 553–559.
Wiesenfeld, K., Moss, F., 1995. Stochastic resonance and the benefits of noise: from ice ages to crayfish and SQUIDs. Nature 373, 33–36.